Journal of
Applied Remote Sensing

RemoteSensing.SPIEDigitalLibrary.org

Analysis of the impact of wavelength separation on reflectivity error for differential absorption lidar using the ASTER spectral library

William D. Tandy, Jr.
Jarett Bartholomew
William J. Emery
Ashwin Yerasi

SPIE.

William D. Tandy, , Jr.Jarett Bartholomew, William J. Emery, Ashwin Yerasi, "Analysis of the impact of wavelength separation on reflectivity error for differential absorption lidar using the ASTER spectral library," *J. Appl. Remote Sens.* **11**(3), 036008 (2017), doi: 10.1117/1.JRS.11.036008.

Analysis of the impact of wavelength separation on reflectivity error for differential absorption lidar using the ASTER spectral library

William D. Tandy Jr.,[a,*] Jarett Bartholomew,[b] William J. Emery,[a] and Ashwin Yerasi[a]

[a]University of Colorado Boulder, Ann and H.J. Smead Aerospace Engineering Sciences Department, Engineering Center, Boulder, Colorado, United States
[b]Ball Aerospace & Technologies, Boulder, Colorado, United States

Abstract. An investigation of the sensitivity of a gas-detecting, airborne differential absorption lidar to the wavelength-based reflectivity variations of the ground was made using the Jet Propulsion Laboratory's (JPL) reflectance library. The JPL library contains 2287 data sets of reflective materials covering a wide range from manmade to lunar regolith. The study covered an online wavelength range of 400 to 4000 nm. Two assumptions were made to provide a path to analysis. The first was that an instrument developer could tolerate no more than 5% error on the overall answer due to reflectivity differences from wavelength separation. The second was that, regardless of atmospheric conditions, molecular cross section, starting power levels, or myriad other effects, the offline received signal is 10% higher than the online received signal. From this foundation, wavelength separation limits were determined when 99%, 95%, and 90% of the materials in the database met the error criteria. It was found that most applications need wavelength separations within about 0.5 nm for low error while some applications could use wavelengths separated by 10 nm or more. Example case studies are provided to demonstrate the applicability and use of the computed plots intended for informing early-stage instrument design. [DOI: 10.1117/1.JRS.11.036008]

Keywords: advanced spaceborne thermal emission and reflection radiometer; differential absorption lidar; IPDA; laser; reflectance; reflectivity; ASTER.

Paper 170330 received Apr. 20, 2017; accepted for publication Jul. 18, 2017; published online Aug. 19, 2017.

1 Introduction

Differential absorption lidar (DIAL) instruments for gas detection send two wavelengths through a medium of interest.[1,2] One wavelength is tuned to be absorbed by the medium of interest (i.e., CO_2, CH_4, O_2, etc.) and is called the "online wavelength." The second wavelength is tuned to be relatively weakly absorbed by the medium of interest, but nearly equally absorbed by other constituents within the signal's path. By measuring the relative losses of the two signals, a measurement of the quantity of the medium of interest can be made.

Starting with the first DIAL instruments, a driving motivation keeping the two wavelengths "closely spaced" has been primarily twofold: first, a concern for the interaction of the lasers with the atmosphere and effects such as backscatter and Rayleigh scattering and, second, a concern for the reflectivity of the targets that the signals are bounced off.[1,2] In the first case, Schotland published an early error analysis on the topic of atmospheric interaction and found that the spectral variation in backscatter and absorption over wavelength deltas of a few tenths of a nm were negligible.[3] Browell et al. extended this result with a paper on the impact of wavelength separation on ozone interaction in the ultraviolet ranges.[4] They found that the worst-case errors were

*Address all correspondence to: William D. Tandy, E-mail: wtandy@gmail.com

1931-3195/2017/$25.00 © 2017 SPIE

less than 10 ppbv between the wavelengths of 286 and 298 nm, or roughly 10% of their original signal, while in some cases the error was less than 1%. Indeed, modern DIAL systems operating in the ultraviolet range continue to be designed with several nanometers of wavelength separation, even though Rayleigh scattering effects are more pronounced at the shorter wavelengths.[5]

The second case of wavelength-based reflectivity variations is a critical part of the DIAL design as the amount of laser energy reflected strongly impacts the signal-to-noise ratio and thus the overall confidence intervals of the result.[6] The effects can be simply addressed through engineered retroreflective targets or, in the case of airborne systems, influence the instrument's behavior through wide ranging surfaces both manmade and natural.[6–8] The desire for nearly equal reflectivity values comes as a result of the gas detection form of the DIAL equation, shown as

$$n_c = \frac{1}{2\Delta\sigma_c(R)}\frac{d}{dr}\ln\left[\frac{N_S(\lambda_{\text{off}},R)-N_B(\lambda_{\text{off}},R)}{N_S(\lambda_{\text{on}},R)-N_B(\lambda_{\text{on}},R)}\right]-\frac{1}{2\Delta\sigma_c(R)}\frac{d}{dr}\ln\left[\frac{\eta_d(\lambda_{\text{off}})\cdot\eta_r(\lambda_{\text{off}},R)}{\eta_d(\lambda_{\text{on}})\cdot\eta_r(\lambda_{\text{on}},R)}\right]$$
$$-\frac{1}{2\Delta\sigma_c(R)}\frac{d}{dr}\ln\left[\frac{\rho(\lambda_{\text{off}})}{\rho(\lambda_{\text{on}})}\right]-\frac{1}{\Delta\sigma_c(R)}[\alpha(\lambda_{\text{on}},R)-\alpha(\lambda_{\text{off}},R)], \quad (1)$$

where n_c is the number density of the gas, N_S is the number of signal photons, N_B is the number of background photons, $\lambda_{\text{off,on}}$ are the offline and online wavelengths, R is the altitude above the ground, η_d is the quantum efficiency of the detector, η_r is the optical efficiency (including geometrical overlap), ρ is the reflectivity of the ground (or target), $\alpha(\lambda,R)$ is the extinction coefficient and contains both the scatter and absorption terms, and $\Delta\sigma_c$ is the difference in absorption cross section for the gas constituent.

The first term is the near-standard form of the equation used in practical operations.[9] To simplify to that level, instrument operators note that the natural logarithm terms in the full equation reduce to zero if their argument is one. Systems are therefore designed to make the online and offline values for each of the arguments as equal as practical. For instance, the second term represents the mechanical and electrical aspects of the instrument design, which cancels to zero if both wavelengths travel through the same medium and are measured by the same instrument. The third term is the reflectivity experienced by the two wavelengths and is the focus of this paper. The fourth term relates to the way the laser pulses are affected by the atmosphere. As discussed above, by assuming that the pulses have "low" wavelength separation and all other factors being equal, the terms are often considered close enough to cancel.

For the reflectance term, the implicit assumption often made is that the offline wavelength has nearly the same reflectance properties as the online wavelength.[2,3,6,8] In fact, extensive paper searches covering built and operated DIAL instruments rarely turned up more than a passing discussion of ground reflectivity. The one relatively modern discussion found was started in an Ehret et al. 2008 paper.[6] There, they investigated a range of theoretical impacts on instrument performance for a space-based, integrated path DIAL CO_2 mission. In their analyses, they assumed that the difference in reflectivity divided by the reflectance of the online wavelength (dp/p) was less than 10^{-4}. From there, the discussion took a tangential direction.

Amediek et al.[7] followed up on Ehret's theories by flying airborne campaigns investigating ground reflectance for lasers with wavelengths near 1.57 μm. They observed that reflectance can vary significantly at a variety of spatial scales over both terrain and water. They calculated between 13% and 54% reflectivity differences for a 50-km flight path taken over snow free and partly snow-covered ground assuming a 10-m pulse-to-pulse ground separation distance. Averaging 350 measurements reduced the error to less than 0.11%. Spatial reflectivity was also the subject of a 2010 effort by Lawrence et al. where quantitative analysis using surface reflectance maps showed that the error contributions from mountains and coastlines may exceed 1%.[10]

The paper found to be closest to addressing the wavelength-based reflectance of the surface is the 2016 study by Spiers et al. on the Jet Propulsion Laboratory's (JPL) 2.05-μm laser spectrometer and its interaction with snow-covered surfaces.[11] In their quantitative study of data collected in operations, they determined that the materials they fly over can have nearly order of magnitude variations in reflectance. Their resolution is even high enough to be able to estimate the relative ages of the snow as older snow tends to be coarser with higher reflectance

values. Unfortunately, their discussion of how wavelength changes might affect the outcome is limited to a brief comparison of trends with 1.57-μm systems and a statement that the general trends in bidirectional reflectance distributions should be similar.

Although not specifically investigating the relationship between online and offline wavelengths and reflectivity, these works do highlight the impact that varying reflectivity can have on the final result and that it may not be negligible. Other authors have also made advances by demonstrating that single-wavelength systems see improved classification results when considering intensity variations due to surface reflectivity.[12,13] For example, Burton et al. used measured reflectivity data to demonstrate that quartz-rich sandstones are more reflective than clay-rich mudstones at their wavelength of 1500 nm. If everything else about the instrument is consistent, then sweeping the beam over terrain and observing intensity variations in the signal allow them to narrow down the potential materials they are reflecting off. Papers such as these hint at the potential real-world influence of reflectivity on multiple wavelength systems but do not touch on the differences in reflectivity over a wavelength range.

In spite of the apparent lack of published analysis on wavelength-based variations in ground reflectivity, an ability to quantify their impact may be useful as there are cases where being able to choose an offline wavelength "far" away from the online one may be beneficial. For instance, there would be advantages to sending both the online and offline pulses at the same time: it cuts down on the differential terrain response between pulses for moving instruments and interfering atmospheric structures along the path would be temporally and spatially identical. However, sending both pulses at the same time can be difficult to implement if the online and offline pulses are close enough that wavelength separating optics in the receiver become problematic. Additionally, systems that measure more than one constituent with multiple wavelengths may benefit from having one offline signal common to multiple online signals. For instance, there are regions where both H_2O and CO_2 absorption peaks are nearby.[14] A system able to measure both molecules concurrently would be collecting data on the two most important greenhouse gases with a single instrument.[15] Finally, although not exhaustively, there may be a particularly attractive online wavelength for myriad reasons, but the nearest offline wavelength could be nanometers away.[14] It may be that, even though the separation is far, the reflectivity is favorable, so the instrument design process can move forward. Converse to the positive examples, it may be that the reflectivity variation gradient is particularly bad in the wavelength region of interest, so even common assumptions about sub-nm separation are not as robust as expected. Several of these specific examples are addressed in the applications section of this paper.

The primary goal of this paper is to provide plots that may be useful to instrument designers interested in a first-cut guideline on how reflectivity may impact their wavelength selection. The database used to generate the plots is also freely available, so, if an interested analyst would like specific results for their application, the same analysis process can be used to do so.

2 Data

The reflectivity data used in the analysis came from the JPL Advanced Spaceborne Thermal Emission and Reflection Radiometer (ASTER) spectral library.[16] The library has over 2400 unique materials and is built from three different data sets with contributions from JPL, Johns Hopkins University, and the United States Geological Survey Spectral Library. The library is comprehensive and "includes spectra of rocks, minerals, lunar soils, terrestrial soils, manmade materials, meteorites, vegetation, snow, and ice covering the visible through thermal infrared wavelength region ($0.4 - 15.4$ μm)."[16]

The data are organized by type (i.e., rocks and vegetation), then by class (i.e., igneous, metamorphic, and sedimentary), and finally by material name (i.e., granite and basalt). Other material libraries exist, such as the ISRIC World Soil Information Database, but they are excluded at this time to focus on the ASTER materials.

The data were brought into MATLAB®, taking care to catch miscellaneous issues such as having multiple reflectance values for the same wavelength, identifying data points with non-numeric values, and finding data sets that began with nonsensical wavelengths of 0 μm. Another issue was that most files were "reflectance versus wavelength" while some were "transmission

versus wavelength." The transmission files, of which there were 158, were removed, leaving 2287 reflectance datasets.

Within this remaining set, there are a number of recurring materials. Duplications most often occurred within the "minerals" type. For example, "calcite" had samples with origins from both England and Italy. The other primary duplication was in having one type named "rocks" and one named "rock." Johns Hopkins University produced the former and JPL the latter. Each had igneous, metamorphic, and sedimentary classes with duplications within the duplications. For example, each igneous class had multiple basalt entries. These types of duplications were merged into consistent type, class, and material names to create the final unique set. For instance, the types rock and rocks became just rocks and calcite was sorted into calcite 1, calcite 2, and so on to keep the subtle variations without confusing the data mining code. Table 1 provides a breakdown of the types, classes, and the number of relevant datasets.

Clearly, not all types and classes are equally relevant for all DIAL applications. Stony meteorites and lunar soil samples are important but not for airborne applications seeking CO_2 or methane. Therefore, in the analysis section we look at breaking the data down further into additional groups.

Important for all datasets is that data in the ASTER library cover two spectral regions: 0.4 to 2.5 μm and 2.0 to 15.4 μm. Detailed information on their data collection methods can be found in the Baldridge ASTER paper, but, briefly, they use gold as their reflectivity standard between database sources and water/pyrophyllite for the visible and infrared regions, respectively, within

Table 1 Type and class listing of the reflectance datasets. For compactness, the meteorite and minerals classes are summarized.

Types	Classes	# of datasets
Manmade materials	Road asphalts and tar	5
	Concretes	5
	General construction	28
	Roofing materials	18
Stony meteorites	Six classes	60
Rocks	Igneous	226
	Metamorphic	114
	Sedimentary	129
	Intermediate	4
Soils	Terrestrial	52
	Lunar	17
Vegetation	Grasses	2
	Trees	2
Water	Distilled water	1
	Sea water	2
	Tap water	1
Frost, ice, and snow	Frost	1
	Ice	1
	Snow	3
Minerals	19 classes	1616

the JPL data set.[16] In the 0.4- to 2.5-μm region, a single pass monochromator with a diffraction grating is used to collect data on a 1-nm scale from 400 to 800 nm and a 4-nm scale from 800 to 2500 nm. In the 2.5- to 15-μm region, a spectrometer with an integrating sphere took 1000 scans with a wavenumber delta of 4 cm^{-1} over a span of 15 min with background measurements being subtracted in postprocessing.

For our analysis, results are presented for two wavelength ranges: the first is 400 to 2500 nm and the second is 2500 to 4000 nm. The first is designed to fall within the range of the data's natural boundary. The second picks up where the first left off and ends above where most DIAL systems operate. Although there are likely to be systems that operate at wavelengths longer than 4000 nm, the trends are similar so that extending our analysis is a case of diminishing returns.

Within the datasets, the spectral library has varying wavelength resolutions. Sometimes sub-nm resolution is available while, in others, tens of nm is available. The wavelengths of the data are not consistent either as some data is available at, for example, 3.9800 μm while others are at 3.9817 μm. To provide a consistent analysis, we used interpolation to align the analysis wavelengths. A trade study showed that MATLAB's Piecewise Cubic Hermite Interpolating Polynomial (PCHIP) interpolation scheme nicely rounded some of the peaks in the data with less than $0.01 \pm 0.02\%$ error relative to a linear interpolation.[17] However, to avoid the appearance of smoothing with data that are not real, the linear interpolation scheme was kept. Instrument designers looking to run their own analyses may want to run a PCHIP interpolation to determine if rounding some of the sharply pointed peaks is desirable for their effort.

A final point worth discussing for the database is that the number of materials within each range varies. The plot in Fig. 1 shows large steps with the most data in the 2100 to 2500 nm range. Above 2500 nm, the number of materials drops to 1365 and maintains that level throughout the rest of the datasets. The large steps are a natural result of combining databases from various organizations with different motivating interests.

The spectral data for absorption were taken from the Pacific Northwest National Labs' (PNNL) database.[14] Their datasets are typically offered in several different temperature ranges. For this analysis, the 25°C files were used and no pressure broadening or other effects were attempted. The goal is to provide general trends, and it is expected that instrument developers likely will use their own absorption line values relevant to their specific application.

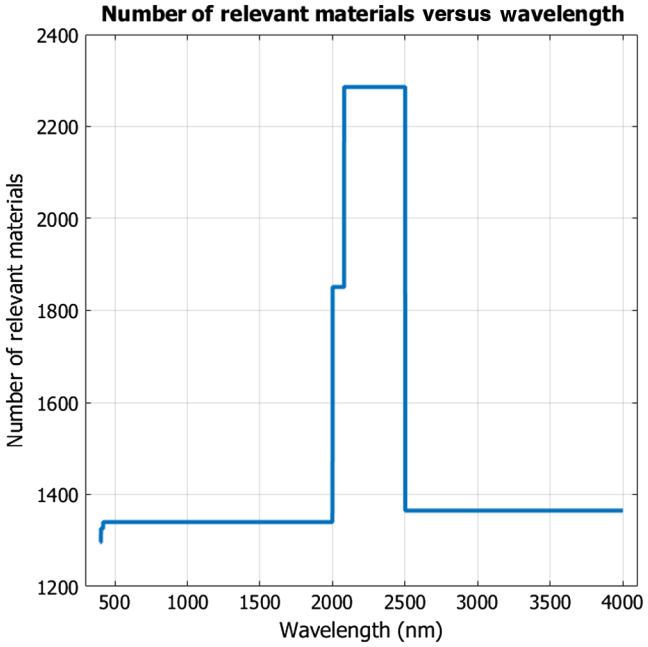

Fig. 1 The number of materials in the database changes with the instrument and organization creating the material information.

3 Methodology

The first step in judging the acceptability of reflectance variations is to set a goal. For this analysis, the assumption is that an instrument developer would be satisfied with a 5% or less error contribution on the final gas concentration measurement due to reflectance variations of the online and offline wavelengths. This number was chosen based on a 1% error possibly being considered negligible or in the noise and 10% feeling like too much of an impact. It was felt that 5% was near the threshold of being important enough to warrant extra attention. Instrument developers interested in tighter error bounds can expect shorter allowable wavelength deltas from those shown in the results section.

Next, as can be seen from Eq. (2), the reflectance contribution is a subtraction from the power ratio; thus, the 5% threshold is a moving target. Therefore, the power ratio must be fixed for consistent analysis. Because molecular cross section, atmospheric environment, and other factors contribute to the received power ratio, the authors recognize that choosing a value is fraught with difficulties. Indeed, infinite combinations of transmitted power and percent absorption can result in the same ratio. As a starting point, however, a received offline power of 10% greater than the received online power is assumed. This value was chosen based on assuming nearly equal offline and online transmitted powers and that the selection of an online wavelength is made such that roughly 9% of the signal is absorbed in typical operations to provide a clean signal. Developers anticipating less online absorption can expect tighter restrictions on delta wavelength because the log ratio that the 5% error is measured from is reduced. Likewise, anticipating greater absorption allows for relaxed wavelength separation limits.

For the nominal case of equal transmitting power, a 9% online wavelength absorption, and a 5% error tolerance, we can express the acceptability threshold as

$$\ln(1.1/1.0) \times 0.05 = 0.0048. \tag{2}$$

This 0.0048 threshold is applied by first taking the natural log ratio of an offline-to-online reflectance pair and then comparing the result against the threshold. If the value is equal to or less than 0.0048, then the error imposed by wavelength-dependent reflectance is less than 5% for the stated conditions. Values higher than this threshold mean that reflectance variations are likely to introduce appreciable noise in the final result. Note that factors other than wavelength-based reflectivity may also impact the final result since effects, such as Rayleigh scattering, are ignored in our analysis.

Three cases are presented in the analysis results section: the first demonstrates the concept of equal reflectivity not necessarily needing to come from nearby wavelengths, the second looks at all of the possible online and offline wavelength combinations, and the third investigates a narrower region around a spectrum of online wavelengths. The second case is useful for the big picture view of the design space while the third is intended to be useful to designers looking for early-stage feedback on wavelength selection. In both of the latter cases, the plots are created by selecting an online wavelength and then calculating the natural log of the offline-to-online ratio for many different offline wavelengths.

Within the last two cases, the first uses an online wavelength that is incremented by 1 nm and an offline wavelength that is incremented by 0.5 nm to create just under 26 million offline-to-online ratios. In the second, the online wavelengths are incremented by 0.1 nm and the offline wavelengths are incremented by 0.05 nm within a range of -6.0 to $+6.0$ nm from the online wavelength to create a little over 8.7 million analysis cases. Both sets were processed using MATLAB's Parallel Processing Toolbox on an Intel i7-930 CPU with 6 GB of RAM, taking about 12 and 4 h, respectively.

For the latter case, the next step was to determine how far the online and offline wavelengths could be separated. Thresholds of the percentage of materials were set and the separation distance between wavelengths were determined that met these thresholds. The percentages chosen were 90%, 95%, and 99%, which mean, for instance, that 90% of the materials in the database would introduce 5% or less error for the calculated separation distance. These latter plots are intended to provide more specific guidance to instrument developers seeking information about trends at their wavelengths of interest.

The final step taken is to present the results by type. The first group is all materials and simply represents all of the materials in the database. The second is a grouping of the rocks, minerals, and soils types. Within this set, the soils type had the lunar regolith class removed and the stony meteorites were removed from the rocks type as these were not deemed practical materials for most DIAL instruments. The third group consists of the water-based types of snow, ice, frost, and water. The vegetation type would be of keen interest, but it only has four samples and so is not further analyzed. Likewise, the manmade materials group suffers from only having 56 samples, which is not comprehensive enough to justify inclusion.

After the plots of the various results, a brief study is made of the impact of choosing different parameters for the error threshold. Instead of the offline-to-online signal power ratio of 1 : 1 and an allowable error contribution of 5%, a range of the two values are compiled for a given wavelength. The wavelength chosen is 1645.55 as it is used in two recent methane DIAL systems and is also the peak absorption value for methane in the near-infrared.[6,8]

4 Analysis Results

Analysis of individual materials shows that there can be wide swaths of wavelengths where the reflectance of a material would support hundreds or even thousands of nanometers of wavelength separation. The plot in Fig. 2 shows the reflectance of marble with the solid line highlighting ranges from which online and offline wavelengths could be chosen while meeting the 5% error contribution criteria. It is seen that, for single materials, satisfying the assumption of equal reflectance can be relatively straightforward.

Extending the single material analysis, a comparison of all wavelength combinations for all of the materials in the database in the wavelength region of 400 to 2500 nm is presented in Fig. 3. The contour plot is divided into 10% contours over the range of 10% to 100%. The region within a contour means that the offline and online combinations therein will provide 5% or less error due to assuming equal reflectance. The outermost contour is the 10% line. Two insets demonstrate some of the fine grained structure within the dense region of the plot.

It can be seen that, although the central diagonal line is narrow, some online wavelengths can tolerate a wider range of offline values. The regions where abrupt changes in the trends are observed, such as near 2.0 μm, are primarily due to the numbers of materials with values beginning/ending at those points. It is worth noting that the percentage is never 0%. There is always at least one material in the database where a given online and offline wavelength combination could work with it as a reflective target.

While Fig. 3 shows a texture of material reflectivities and the complex nature of photon and molecule interactions, it is somewhat impractical in practice. In an effort to create plots useful for

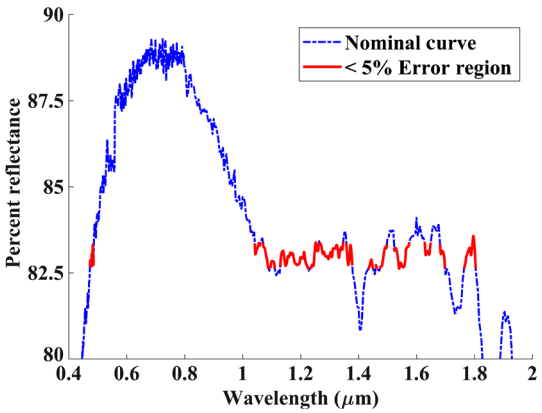

Fig. 2 The distribution of reflectance (%) with wavelength. Many materials, such as the marble shown here, have multiple wavelengths over a wide range with similar reflectance. The solid line highlights are wavelengths that would produce less than 5% error in the overall DIAL result for a nominal 83% reflectance.

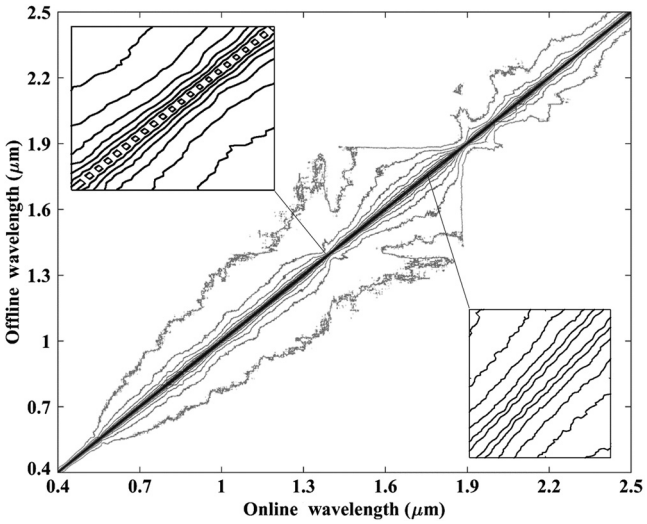

Fig. 3 Contour plot of the percentage of materials within the JPL library that introduce less than 5% error in a DIAL signal. Contours are in 10% increments, starting with 10+% at the outermost contour and ending at 100% in the innermost regions. Insets demonstrate some of the fine-grained structure in the dense, central region.

instrument designers, a tighter range of offline wavelengths, specifically 0 to 6 nm around the online wavelengths, are presented next. As described in the methodology section, the values of 90%, 95%, and 99% mean that, for instance, 90% of the materials in the database meet or improve on the 5% error threshold while 10% of the materials would induce errors greater than 5% of the overall signal. Because the allowable ranges are not symmetric about a given online wavelength, the minimum distance is used from either direction. This simplification sacrifices a mean absolute differential of 0.12 ± 0.21 nm while allowing for more detail in these already large plots. The simplification means that the plot is conservative by this amount, so, if a particular application is on the cusp of acceptability, it may be that analysis expands the envelope.

Performing this computation for all materials and the "Minerals, Rocks, and Soil" grouping showed nearly identical results. The mean difference in allowable offline separation for the 90%, 95%, and 99% thresholds are 0.04 ± 0.04, 0.02 ± 0.02, and $0.01 \pm .01$ nm, respectively, which are smaller than the 0.1-nm resolution of the database. Visually, it was not possible to differentiate the two without zooming in to levels not relevant to publishing. As 2139 of the 2287 materials in the database fall within the minerals, rocks, and soils types, this is not a surprising result. To save space through reduced image count, and because we hope to extend this work in the future with more manmade and vegetation data, the latter plot is retained and the former saved for a time when more materials may differentiate it from the latter.

It is seen that the results are not uniform. In particular, the results above 2 μm in Figs. 4 and 5 plummet. The source of this behavior is found in Fig. 1, where the number of database materials above 2 μm jumps considerably. Many of the materials in this range also have very low reflectivities. For instance, the mineral talc begins at 2.08 μm with 2.9% reflectivity, briefly jumps above 3% reflectivity at 2.083 μm, then immediately falls below 2.9%, and does not exceed it again until about 8.3 μm. Low reflectivity materials are challenging in this percentage-based success criteria as a reflectance change from 5% to 4% is a larger percentage change than 90% to 89%.

For the water-centric categories, although there are various forms of water present in the database, it is still a single molecule; the 99% threshold is the only threshold provided as the other thresholds are equivalent. It is seen that, if an instrument is designed to primarily interact with water, snow, or ice, there can be broad differences in the wavelengths (Figs. 10 and 11).

Throughout the paper, an offline-to-online ratio of 1.1 has been used with an allowable error contribution due to wavelength-based reflectivity variations of 5%. To demonstrate the

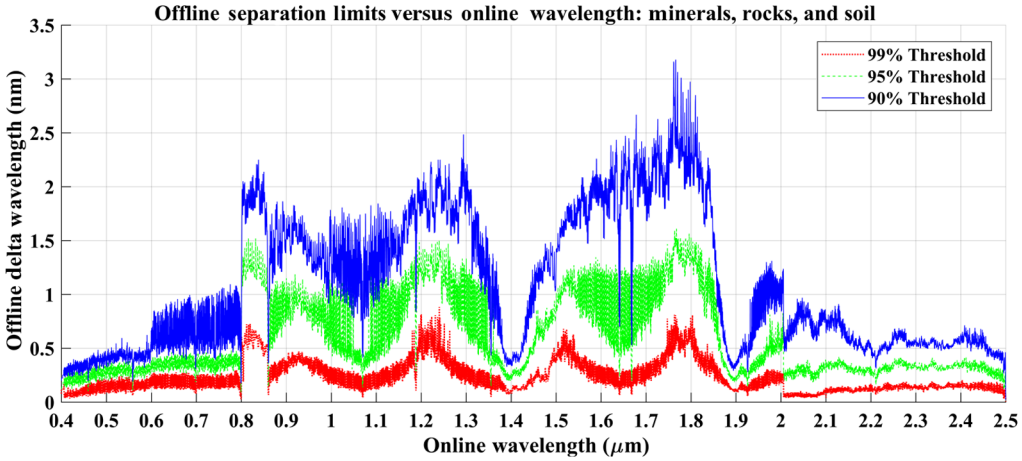

Fig. 4 Absolute values of the offline wavelength regions for various thresholds for the wavelength region from 400 to 2500 nm. The top contour is the 90% threshold.

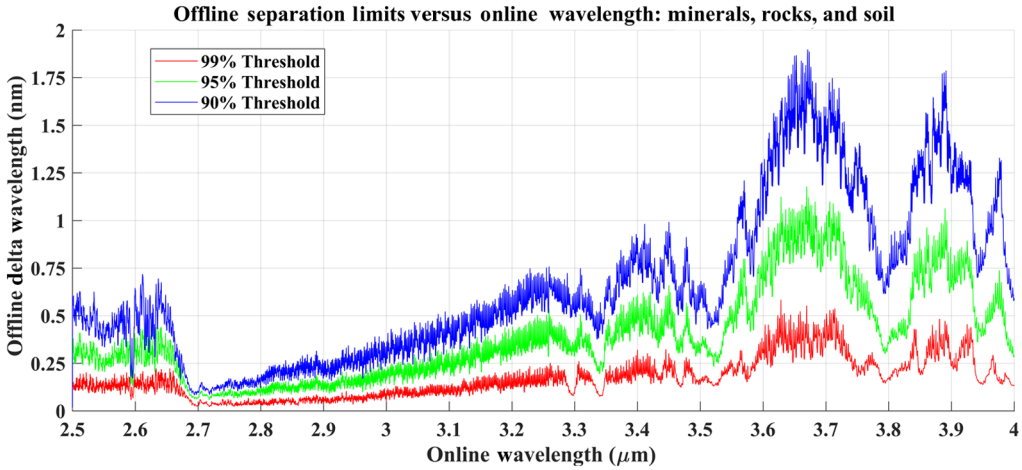

Fig. 5 Absolute values of the offline wavelength regions for various thresholds for the wavelength region from 2500 to 4000 nm. The top contour is the 90% threshold.

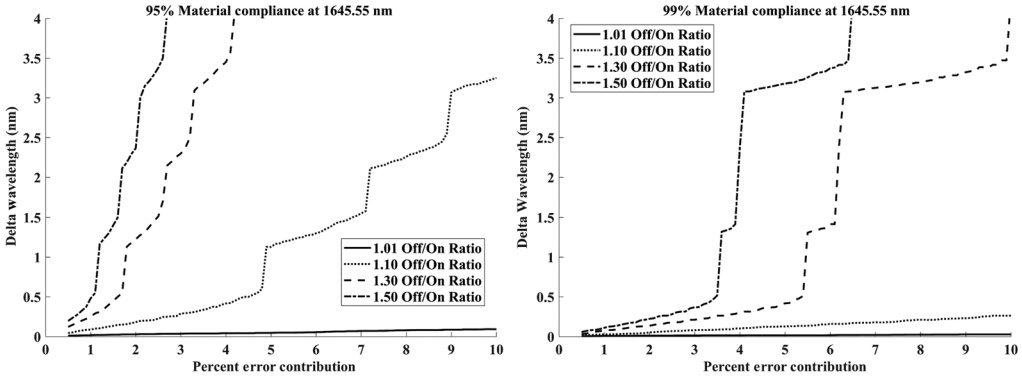

Fig. 6 Sensitivity plots of the allowable percent error contributed by reflectivity variations with each line representing the ratio of offline to online received power. The nominal case used throughout the paper is 5% error with a ratio of 1.10.

sensitivity of the analyses to these values, Fig. 6 plots the ratios and percentages for a wavelength of 1645.55 nm. The plot on the left represents the result when 95% of the materials must meet the threshold while the plot on the right does the same for 99% of the materials. It is seen, for instance, that asking for 99% of the materials to contribute 1% or less error is virtually impossible with only about 0.06 nm of allowed offline separation within the threshold. On the other hand, larger wavelength separations are allowed if a system has a higher than the 1.1 offline to online signal power ratio used for the plots in this paper. Overall, the conclusion is that the error threshold relationship is not linear and a specific application will benefit from customized analysis. Also, instruments seeking no error from reflectivity variations either need very tight offline to online separation or a design with an eye toward significant online absorption. It is likely that a system will encounter at least a couple of percent error even with tight design requirements.

5 Example Applications

Two example preliminary designs are provided to demonstrate how the plots above may be used to influence an initial wavelength choice. The first case studied is for an airborne instrument seeking to detect methane in the atmosphere. The instrument designer begins by noticing that there are three main clusters of methane absorption lines below 4 μm. The peak absorptivities from these three regions are pulled and compared with the reflectivity data. The result is shown in Fig. 7. The plots show that the first and third cases have strong potential with order of magnitude drops in absorptivity within the 99% regions and further reductions in absorptivity within the 95% regions. However, the 2.370-μm region is noisy, and it is not until the 90% region that a decent offline wavelength becomes available, according to reflectivity, even though it is less than 0.5 nm away.

The second, more complex, application is a DIAL instrument seeking to measure both CO_2 and H_2O concentrations using a shared offline wavelength. In this example scenario, perhaps a low altitude unmanned aerial system is flying over arid deserts or polar zones (where water concentration is low) seeking to measure two of the most important greenhouse gases.[15] The instrument designer starts by scanning the PNNL spectral absorption library and finds that there are two promising regions where the peaks of absorbance values of the two gases are near each other and there is potentially a reasonable nearby offline to warrant further consideration: 1.956 and 2.708 μm. In the first case, there are many lines within a 2-nm region with a nearby order of magnitude drop in absorptivity, indicating a potentially good offline selection. In the second case, there is only one peak for each gas, but they are within 0.9 nm of each other and there is more than an order of magnitude drop in absorptivity in their valley.

One of the next steps would be to then consider the potential impact that ground reflectivity would have on the results. The 1.956-μm wavelength region is shown in Fig. 8. There, the CO_2 and H_2O absorption lines are shown with the vertical bars representing the percent of materials that would introduce minimal error due to reflectivity errors. It is seen in this example that CO_2 has two potential peaks and H_2O has one peak within the range where the vast majority of

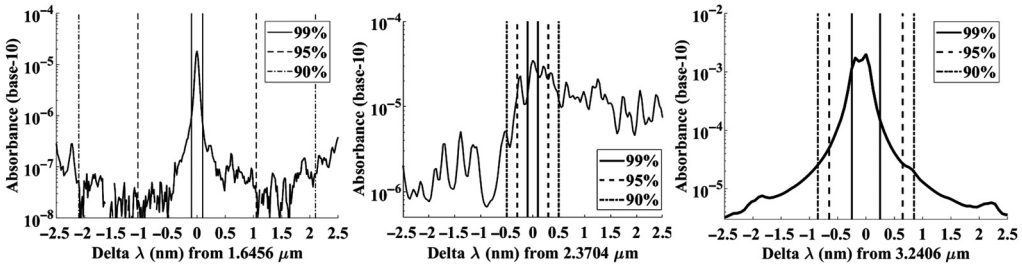

Fig. 7 The center of the three plots represents the peak values from the three main clusters of absorptive online wavelengths for methane below 4 μm. The vertical bars span regions where 90%, 95%, and 99% of all of the materials in the database contribute 5% error or less.

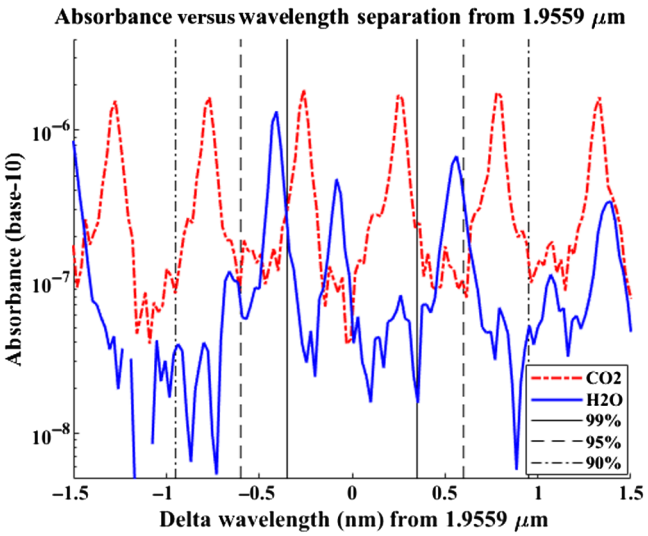

Fig. 8 Plot of the CO_2 and H_2O absorption lines for the first wavelength region considered for the UAV instrument.

materials reflect with minimal error. If the designer feels that the 95% region is acceptable, then two more peaks of H_2O are available.

In the second case, the 2.708-μm region does not fare so well. It is seen in Fig. 5 that the 2.7-μm region is one of the most difficult in terms of reflectivity and that impact is demonstrated in Fig. 9: these two strongly absorbing features may not be suitable for airborne instruments as a significant percentage of materials impose meaningful error into the signals at this wavelength separation.

For the above cases, the central theme is that reflectivity can play a strong role in wavelength selection. The empirical analysis available with spectral libraries such as JPL's ASTER library means that instrument designers can make informed decisions instead of relying on general rules. The precomputed plots in Figs. 4, 5, 10, and 11 can also be used as a first step to more detailed analysis.

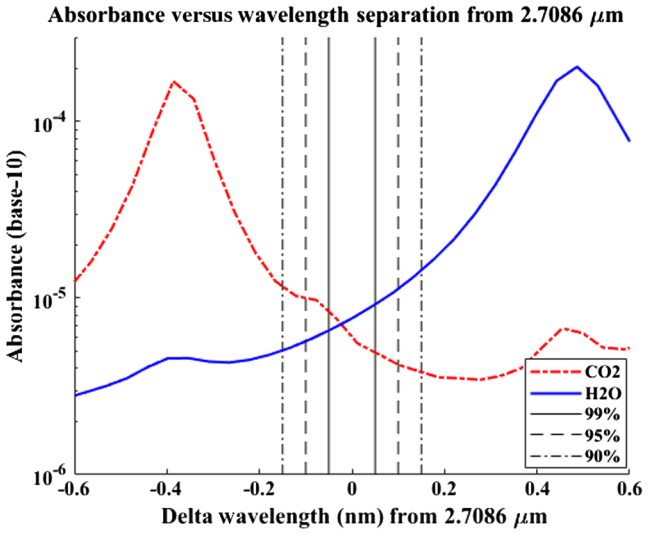

Fig. 9 Plot of the CO_2 and H_2O absorption lines for the second wavelength region considered for the UAV instrument.

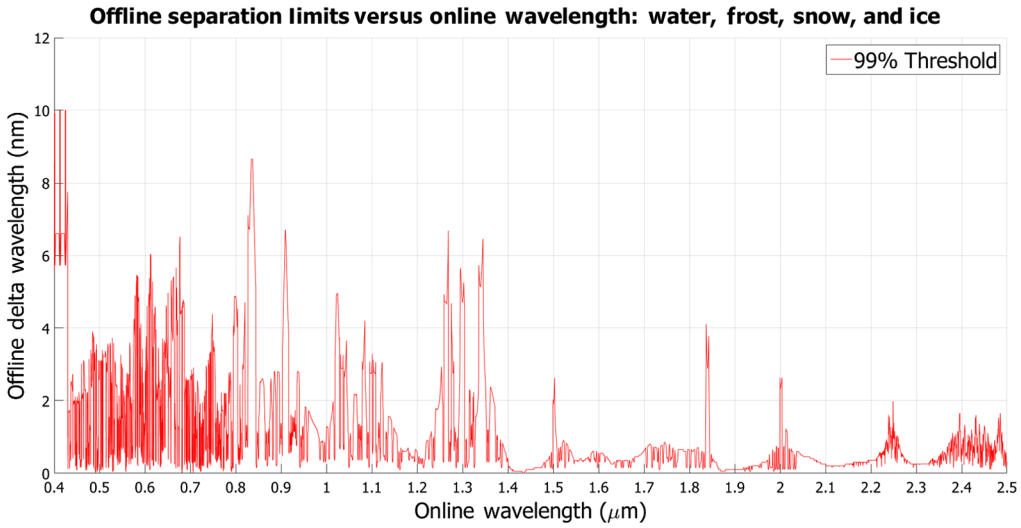

Fig. 10 Absolute value of the allowable offline wavelength separation for the water types, with nine sample sets. The analysis only went to 10 nm of separation, cutting off some of the result around 400 nm.

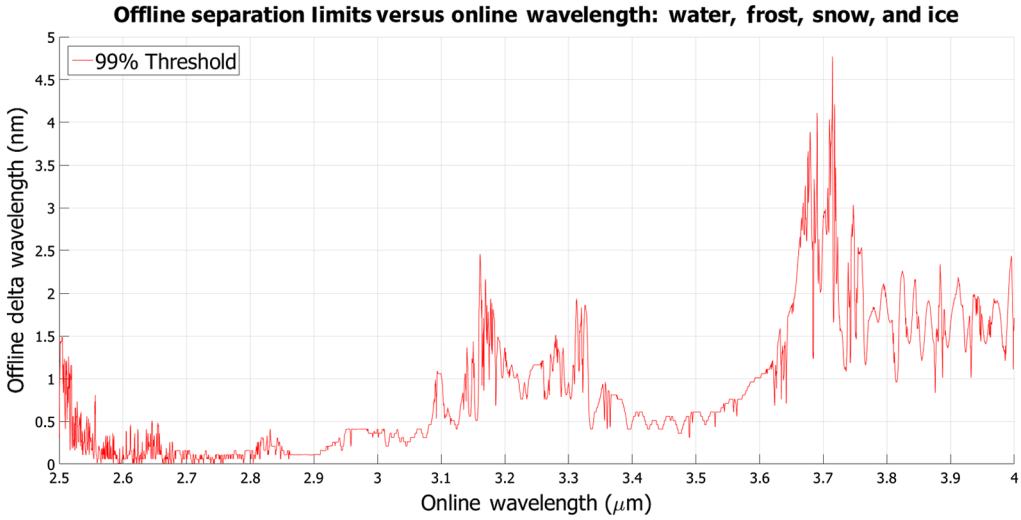

Fig. 11 The plot represents the allowable wavelength separation for the nine water molecules in the database for the 2.5- to 4-μm region. For these two cases, percentages are not relevant as the line represents the threshold for less than 5% error for all forms of the water data.

6 Conclusions

Empirical analyses of thousands of materials have shown that, depending on their application, DIAL instrument developers utilizing unknown terrain to reflect signals may have flexibility in choosing their online and offline wavelengths. In many scenarios, several nanometers of separation may be achievable. In other cases, otherwise desirable DIAL wavelengths are shown to face challenges due to the potential for introduced errors from reflectivity mismatches. Although instrument designers are likely to want to compute specific results for their applications, the plots in Figs. 4, 5, 10, and 11 should prove useful as a first step to understanding the potential reflectivity benefits or challenges at a given wavelength.

One area that would benefit greatly from future work would be extending the spectral library to include more vegetation samples. This is recognized as a challenge as vegetation reflectivity is likely to change with the time of year and moisture content. However, this type of data would be

highly valuable to instrument developers that depend on vegetated ground reflectivity for their return signals. Along the same lines, greater numbers of manmade materials would be useful. In spite of these desired improvements, the authors recognize the great utility of the ASTER spectral library and are grateful for the efforts of its creators.

References

1. R. M. Schotland, "The determination of the vertical profile of atmospheric gases by means of a ground based optical radar," in *Proc. Third Symp. on Remote Sensing of the Environment*, Environmental Research Institute of Michigan, Ann Arbor (1964).
2. R. T. Menzies and M. S. Shumate, "Tropospheric ozone distributions measured with an airborne laser absorption spectrometer," *J. Geophys. Res.* **83**(C8), 4039–4043 (1978).
3. R. M. Schotland, "Errors in the lidar measurement of atmospheric gases by differential absorption," *J. Appl. Meteorol.* **13**, 71–77 (1974).
4. E. V. Browell, S. Ismail, and S. T. Shipley, "Ultraviolet DIAL measurements of O_3 profiles in regions of spatially inhomogeneous aerosols," *Appl. Opt.* **24**(17), 2827–2836 (1985).
5. R. J. Alvarez et al., "Development and application of a compact, tunable, solid-state airborne ozone lidar system for boundary layer profiling," *J. Atmos. Oceanic Technol.* **28**(10), 1258–1272 (2011).
6. G. Ehret et al., "Space-borne remote sensing of CO_2, CH_4, and N_2O by integrated path differential absorption lidar: a sensitivity analysis," *Appl. Phys. B* **90**(3–4), 593–608 (2008).
7. A. Amediek et al., "Airborne lidar reflectance measurements at 1.57 μm in support of the A-SCOPE mission for atmospheric CO_2," *Atmos. Meas. Tech.* **2**(2), 755–772 (2009).
8. J. Bartholomew et al., "Airborne active sensing for pipeline leak survey," in *AIAA Information Systems-AIAA Infotech@ Aerospace*, Grapevine, Texas, p. 0645, American Institute of Aeronautics and Astronautics, Reston, Virginia (2017).
9. T. Fujii and T. Fukuchi, Eds., *Laser Remote Sensing*, CRC Press, Boca Raton, Florida (2005).
10. J. P. Lawrence, R. J. Leigh, and P. S. Monks, "The impact of surface reflectance variability on total column differential absorption LiDAR measurements of atmospheric CO_2," *Atmos. Meas. Tech. Discuss.* **3**(1), 147–184 (2010).
11. G. D. Spiers, R. T. Menzies, and J. C. Jacob, "Lidar reflectance from snow at 2.05 μm wavelength as measured by the JPL airborne laser absorption spectrometer," *Appl. Opt.* **55**(8), 1978–1986 (2016).
12. D. Burton et al., "Lidar intensity as a remote sensor of rock properties," *J. Sediment. Res.* **81**(5), 339–347 (2011).
13. W. Y. Yan and A. Shaker, "Radiometric correction and normalization of airborne LiDAR intensity data for improving land-cover classification," *IEEE Trans. Geosci. Remote Sens.* **52**(12), 7658–7673 (2014).
14. S. W. Sharpe et al., "Gas-phase databases for quantitative infrared spectroscopy," *Appl. Spectrosc.* **58**(12), 1452–1461 (2004).
15. S. Solomon et al., *Climate Change 2007: The Physical Science Basis, Working Group I Contribution to the Fourth Assessment Report of the IPCC*, Cambridge University Press, New York (2007).
16. A. M. Baldridge et al., "The ASTER spectral library version 2.0," *Remote Sens. Environ.* **113**(4), 711–715 (2009).
17. F. N. Fritsch and R. E. Carlson, "Monotone piecewise cubic interpolation," *SIAM J. Numer. Anal.* **17**, 238–246 (1980).

William D. Tandy, Jr. is a PhD candidate in the Aerospace Engineering Department at the University of Colorado Boulder. He received his BS and MS degrees in aerospace engineering from the University of Texas at Austin. In his 15-year career, he has made significant contributions to space-based remote sensing instruments, including the WorldView imaging satellites, NASA's OMPS and LIMB instruments, and the upcoming James Webb Space Telescope. His current research interests include laser and infrared instrument design.

Jarett Bartholomew received his BS degree from Weber State University in applied physics and his MS degree from the University of California, Irvine, in chemical and materials physics. His 17-year career has focused on lasers and their applications in the sciences. His past work includes building the first commercially available guide star lasers for observatories, instruments for biomedical applications, and DIAL systems. Currently, he works at Ball Aerospace as the chief engineer for their methane detection project.

William J. Emery received his PhD from the University of Hawaii in 1975. He was appointed professor in aerospace engineering sciences at the University of Colorado, Boulder, in 1987. He has authored over 190-refereed publications and 3 textbooks. He is a fellow of the IEEE, the American Meteorological Society, the American Astronautical Society, and the American Geophysical Union.

Ashwin Yerasi received his BS degree in physics and astronomy and his MEng degree in space systems engineering from the University of Michigan. He is currently pursuing his PhD in aerospace engineering at the University of Colorado with a focus in remote sensing. His research involves modeling the performance of airborne lidar systems as they are used to detect natural gas leaks.